



Effects of nanocrystalline calcium oxide particles on mechanical, thermal, and electrical properties of EPDM rubber

Nashwan Q. Mahmood^{1,4} · Kálmán Marossy^{1,2} · Peter Baumli³

Received: 27 May 2021 / Revised: 1 August 2021 / Accepted: 16 August 2021 / Published online: 11 September 2021
© The Author(s) 2021

Abstract

In this research, the effect of calcium oxide (CaO) nanocrystalline particles filled ethylene propylene diene monomer (EPDM) rubber composites is investigated, at different weight percentages (1.0, 2.0, 4.0, and 8 wt%) of CaO nanocrystalline particles using two methods of mixing. In one case conventional mixing on twin roll-mill was used, in the other case ultrasonic mixing as a pre-mixing was applied. CaO particles are synthesized by the precipitation method. The average crystallite size of CaO is 100 ± 20 nm. Adding CaO nanocrystalline particles increases the thermal stability of EPDM and the glass transition temperature. The hardness of EPDM rubber gradually increases with increasing the amount of CaO particles, the maximum hardness 64.2 observed in 8 wt% of CaO particles for both cases almost 26% higher than neat EPDM. Tensile strength decreases, while the maximum % modulus of the ultrasonic mixed sample was 1.48 MPa which is 24% higher than EPDM.

Keywords CaO nanocrystalline particles · EPDM · Thermo-mechanical properties · DMA · TGA

Introduction

In materials science, one of the most important phenomena is the reinforcement of rubber by fine, rigid entities, dispersed particulate, or phase-separated domains. To know significant reinforcement, the size of the hard phase should be small, smaller than a micron, reinforcement increases resistance to fracture and stiffness [1]. Filling polymers by a combination of fillers receive continuous interest because of their natural ability to improve heat stability [2], mechanical properties [3], flame retardancy [4], abrasion resistance [5, 6] of the polymer matrix, and gas barrier properties [7]. Carbon black is a conventional reinforcing agent that increases the mechanical and abrasion properties of polymers [8]. Nanoparticles are a unique scientific interest as they are great effectively a bridge

between molecular or atomic structure and bulk materials [9]. Metal oxide nanoparticles are the most important materials due to the great widespread applications some metal oxide nanoparticles (CaO, ZnO, TiO₂, and CeO₂) can use in various aspects including sensors, catalysis, environmental remediation, and optoelectronic materials [10–17]. There are some methods that CaO nanoparticles can be synthesized which include thermal decomposition method [18], solution combustion method [19], microwave processing [20], sonochemical method [15], coprecipitation method [21], and sol–gel method [22]. EPDM (ethylene propylene diene monomer) is a commercially important as unsaturated polyolefin rubber. In general, EPDM compound has excellent chemical resistance to water, ozone, brake fluid, radiation, weather, and glycol. EPDM high resilience is preferred. EPDM is good vulcanizates, providing improved wet electrical properties. EPDM is resistant to oxygenated solvents, salt solutions, and synthetic hydraulic fluids. By a gel-free process when diene vinyl norbornene is mixing on the EPDM backbone, a significantly improved terpolymer is obtained for cable and wire applications. Other applications of EPDM are automotive body seals, mounts, roofing, weather-stripping, hose, ducts, tubing, and tires. EPDM molded rubber is used for fillers and bumpers to get damp vibrations around the vehicle [23–25]. Although the possibility use of polymer nanocomposites in the electrical insulating industry is still in its early stages,

✉ Peter Baumli
fembaumli@uni-miskolc.hu

¹ Institute of Ceramic and Polymer Engineering, University of Miskolc, Miskolc, Hungary

² BorsodChem Zrt, 3700 Kazincbarcika, Hungary

³ Institute of Physical Metallurgy, Metal Forming and Nanotechnology, University of Miskolc, Miskolc, Hungary

⁴ Department of Mechanical Engineering/Production, College of Engineering, Sulaimani Polytechnic University, Sulaimani, Kurdistan, Iraq

polymeric materials offer great benefits in outdoor insulation systems due to their great dielectric properties, better pollution performance, low cost, ease of processing, and lightweight [26]. Mohamed et al. [27] investigated the effect of CaO nanoparticles on the properties of Polyamide6 (PA 6) by adding 0.5% calcium oxide nanoparticles to it using melt compounding HAAKE twin screw extruder. Their result revealed that tensile strength and stiffness increase and elongation at break decrease by adding CaO nanoparticles. CaO nanoparticles improved the thermal stability of the composite. Sunil et al. [28] studied thermal properties of CaO nanofluids, by using CaO nanoparticles as a bio-lubricant, an additive is synthesized from chicken eggshells and dispersed rice bran oil as a base fluid ultrasonicated for 20 min; at 20 kHz using probe sonicator as a mixer, the result revealed that thermal stability of rice bran oil increase by 18.2% and 25% due to the addition of 0.25 wt% and 0.50 wt% of CaO nanofluids, respectively, but it does not affect rice bran oil oxidation behavior. Rana et al. [29] studied electrical, mechanical, and thermal properties of EPDM rubber with different amounts of montmorillonite (MMT) nano clay reinforced (2 wt%, 4 wt%, and 6 wt%); the two-roll mill was used for blending it. Mechanical properties increase with an increasing amount of clay, such as tensile strength, and young modulus, with increasing frequency dielectric constant decrease and conductivity increase. By adding nano clay to the EPDM dielectric constant and conductivity increase and the higher value, it was observed 2 wt% nanocomposites. The value of storage modulus increase significantly, the higher value of thermal stability observed in 2 wt%. Wang et al. [30] studied thermal conductivity and mechanical properties of EPDM rubber with different amounts of nano ZnO reinforced (10, 20, 40, 60, 80, 110, 140, 180, and 210 phr, respectively). Nano ZnO particles enhance better dynamic heat build-up mechanical properties by in situ modification. It can be found a few papers in the literature about the CaO-EPDM rubber composite. The effect of the nanocrystalline CaO on the mechanical behavior of CaO-EPDM rubber composite is not detailed. In this work, we prepare the CaO particles from an aqueous solution. We investigate the structure of the CaO. In the second part of the paper, we are using the CaO particles in EPDM rubber as reinforcement.

Materials and methodology

Materials

Materials used in the present study are ethylene propylene diene monomer (Keltan 778) DSM-LANXESS, with an ethylene content of 67% and ethylidene norbornene (ENB) 4.3%, stearic acid as a lubricant, paraffin oil (Ph.Hg. VIII quality), and triallyl cyanurate (TAC) as a vulcanization

accelerator, which were kindly provided by Borsod ChemZrt. CaO nanocrystalline particles were produced by precipitation method using 1 mol/L of CaCl₂ and 2 mol/L of NaOH as a reactant at the institute of nanotechnology department in the University of Miskolc. Dicumyl peroxide 98% were purchased from (Alfa Aesar). The composition of the material is represented in Table 1.

Sample preparation

Preparation of the calcium oxide particles

In this experiment, CaO nanocrystalline particles have been prepared by precipitation methods. The reactants that were used to prepare CaO is 1 mol/L of CaCl₂ and 2 mol/L of NaOH; first of all, 20 cm³ of CaCl₂ and 20 cm³ of NaOH were heated up to 80 °C on the hot plate of magnetic. NaOH was added dropwise into CaCl₂ at the fixed temperature of 80 °C while stirring continues for 30 min and (1300 rpm) viscously was produced. The precipitate was collected by filtration after rinsed five times with distilled water to remove impurities. In this work, the reactions that occurred are shown at Eqs. (1) and (2).



The white calcium hydroxide (Ca(OH)₂) precipitate was calcined in the furnace at 650 °C after that holding furnace for 1 h at this fixed temperature, finally collecting the nanocrystalline particles CaO and putting them in an airtight container. This method can be used as a cheap, simple, and convenient way for producing calcium oxide and hydroxide nanocrystalline particles in the industrial large scale.

Table 1 Composition of the samples

Material	Composition in parts per hundred rubber (phr)
EPDM rubber	100
CaO nanocrystalline particles	(0, 1, 2, 4, and 8)
Dicumyl peroxide (DCP)	3
Stearic acid	1*
Paraffin oil (PO)	10
Triallyl cyanurate (TAC)	2

*in CaO free base formulation only

Preparation of EPDM rubber/CaO nanocomposites

In this section, the procedure for preparing EPDM rubber/CaO nanocomposite is shown and discussed by using two methods of mixing. First using the conventional way on twin roll-mill adding the components on the molten polymer. The second way starts with pre-dispersing the nanocrystalline particles in the plasticizer oil by ultrasonic vibration. The EPDM rubber was rolled on twin-roll mill with 150 mm in diameter (Schwabenthan 150 U, Germany) at 110 °C temperature at 16 rpm without friction for approximately 5 min. Thereafter the oil (stearic acid if any), CaO nanocrystalline particles, dicumyl peroxide (DCP), and triallyl cyanurate (TAC). In case of ultrasonic mixing, the CaO was dispersed in the plasticizer oil, and this milk like material was added first onto the EPDM felt. It was interesting observation that the ultrasonically mixed CaO containing sheets were not rugged. Finally, the blended rubber/CaO nanocrystalline particle mixtures were compression-molded for the sample preparation of tensile and hardness in 120 mm × 120 mm mold and simultaneously cross-linked for 8 min at 165 °C, using oil-hydraulic pressure 30 bar.

Characterization CaO powder

Scanning electron microscopy (SEM)

Surface morphological features were studied by using (Helios G4 PFIB CXe) scanning electron microscope equipped with a high voltage of 10 kV. The samples were coated with gold to improve the electrical conductivity and reduce the charging for getting good image quality for analysis.

X-ray diffraction (XRD)

The crystallite size and weight percentage of calcium oxide powder were examined by using (Bruker D8 Advance diffractometer) X-ray diffraction (XRD).

$$D = \frac{0.9\lambda}{\beta \cos\theta} \quad (3)$$

where D is the mean crystalline size (nm), λ is the wavelength of Cu K α (0.154 nm), β is the full width at half maximum intensity (FWHM) in radian, and θ is the Bragg angle.

Brunauer–Emmett–Teller (BET)

The specific surface area and the distribution of pore sizes of the CaO nanocrystalline particles calcined

at 650 °C were examined by using (TriStar 3000) Brunauer–Emmett–Teller (BET).

Mechanical characterization

Tensile test

Tensile testing is one of the most basic engineering tests and supplies useful information about a material and its related properties. For engineering structures, these properties can be used for analysis and design and for improving new materials that better suit a specified use [31]. EPDM rubber and different wt% of CaO particles samples were to characterize the material under the tensile loading by using Instron 5566 universal testing machine. In each set, three samples were tested according to ISO 527 standard. The crosshead speed was 100 mm/min. The thickness and width of the tensile samples used were about 1 mm (individually measured) and 4.6 mm, respectively. The gauge length of the specimen used was 25 mm.

Hardness test

Hardness test is defined as hardness resistance of materials against indenter by harder materials. Shore A is used for softer rubbers and soft plastic like plasticized PVC. One advantage of the Shore procedure is its mobile application capability since hand-held devices are often used [32]. In the present study, hardness measurements were made according to ISO 868 standard at 23 ± 1 °C using Shore A hardness tester (Zwick/Roell) machine. Each sample was 3 mm in thickness, and five different positions were tested from each rubber. Arithmetic mean value was calculated.

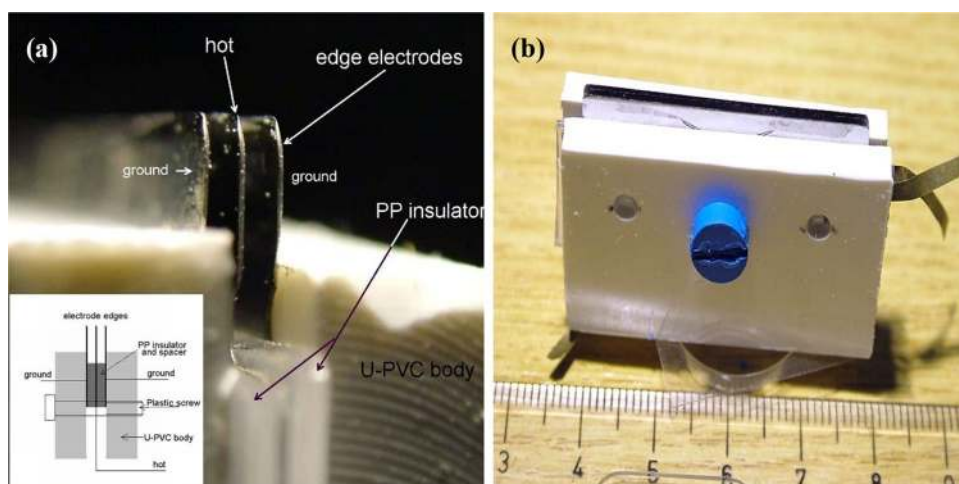
Thermal characterization

In this study, there were two different thermal characterization tests performed for investigating the thermal properties with the help of dynamic mechanical analysis (DMA) and thermogravimetric analysis (TGA).

Dynamic mechanical analysis (DMA)

DMA is a nondestructive test technique in the area of polymer matrix analysis [33]. The thermomechanical behavior of the EPDM samples was characterized by the use of (Metravib 1DB DMA25 instrument) DMA solicitation type: tension–compression over a temperature range of -80 to 80 °C with a heating rate of 2 °C per minute at a frequency of 10 Hz. The thickness and width of the tensile specimens used were 1 mm and 10 mm, respectively (measured by accuracy of 0.05 mm); also the gauge length of the specimen used was 15 mm. It is important to use a low heating

Fig. 1 (a, b) New electrode system for volume resistivity measurement



rate so that the sample can have enough time to achieve the thermal balance within the chamber. As a function of temperature, the storage modulus and the loss factor $\tan(\delta)$ were measured. Glass transition temperatures (T_g) were evaluated as the maximum point temperature of $\tan(\delta)$.

Thermogravimetric analysis (TGA)

TGA is the most commonly used thermal characterization technique to identify information about changes in percent weight of the analyzed specimens as a constant heating rate with respect to temperature or a constant temperature with respect to time [34]. In the present research, thermal stability and mass change of neat EPDM and its nanocomposite as a function of temperature from 40 to 655 °C and constant heating rate 10 °C/min was investigated. The measurement carried out by (MOM Derivatograph-C) instrument.

Volume resistivity

In the present study, the measurements of volume resistivity were observed of neat EPDM rubber and the nanocomposites, by a high-insulation resistance meter device (Danbridge

DB621 Megohmmeter). Volumetric resistivities were evaluated by applying 1 kV to the surfaces of the samples for 60 s; the plate was about 1 to 1.4 mm thick, individually measured. The resistance of the specimens were so high that the measurement was not possible. Therefore, new and specific electrode was made for the present study as shown in Fig. 1 to measure the volume resistivity. The accuracy of this arrangement is less than the standard electrode system, but for comparative study, it is suitable. All of the electrical property measurements were carried out at room temperature.

Results and discussions

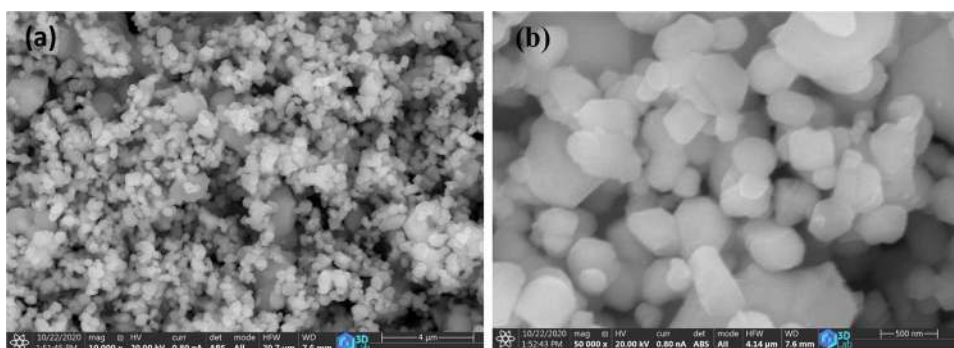
Mechanical, thermal, crystallographic, and electrical properties of neat EPDM and its nanocomposites are discussed in this section.

CaO powder characterization

Scanning electron microscopy (SEM)

SEM micrographs of CaO nanocrystalline particles were taken for two different nominal magnifications, namely

Fig. 2 SEM micrographs of CaO nanocrystalline particles for different nominal magnifications. (a) $M=10\text{ k}\times$, (b) $M=50\text{ k}\times$



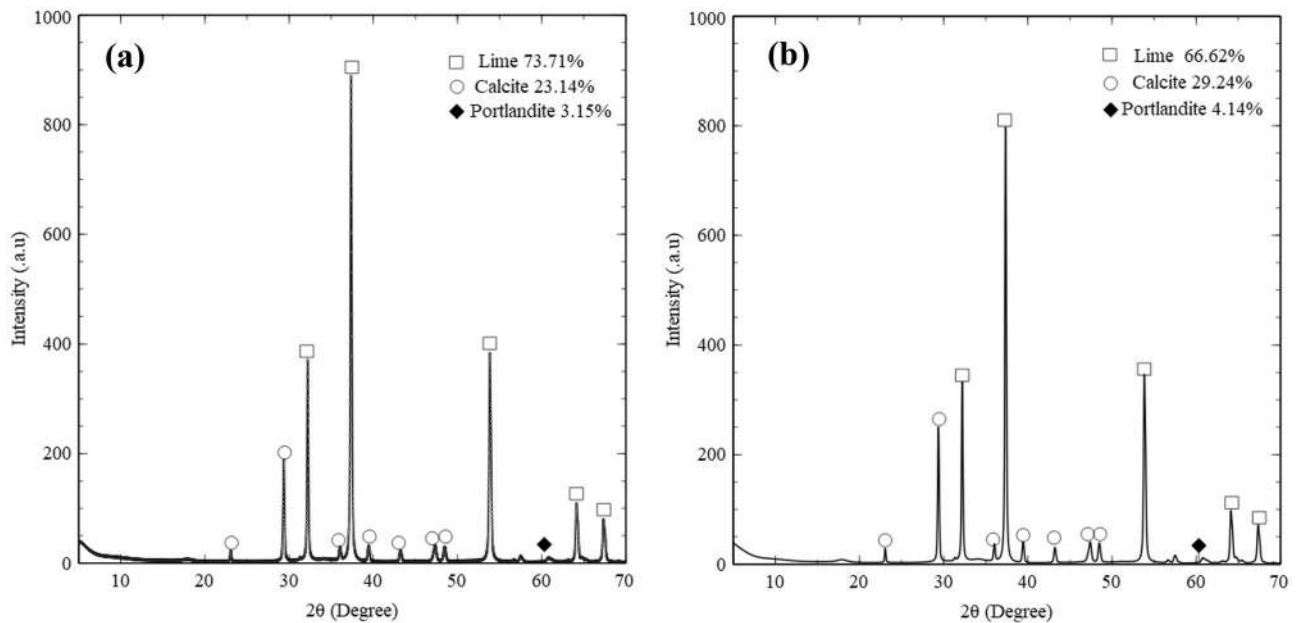


Fig. 3 Powder X-ray diffraction patterns of CaO particles (a) after 1 day and (b) after 1 month

10 k \times , and 50 k \times which are shown in Fig. 2a, b, respectively. SEM micrographs of CaO nanocrystalline particles showed that mainly the spherical shape and average size of nanocrystalline particles was 280 nm.

X-ray diffraction (XRD)

Powder X-ray diffraction (XRD) was used to analyze the crystallographic structure of the synthesized specimens,

the crystallite size, and the weight percentage of calcium oxide powder. The analysis was observed with the help of (Bruker D8 Advance diffractometer) X-ray diffraction (XRD). It's revealed that from Fig. 3a, b, that Ca(OH)₂ after calcination at 650 °C for 1 h remain CaCO₃ because the reaction of carbonation happen fast for Ca(OH)₂ and CaO by atmospheric CO₂ and increasing specific surface area those are reported in the literature [18, 35]. The predominant peaks happen around $2\theta = 37.5^\circ$, and the average crystallite sizes were estimated from line broadening

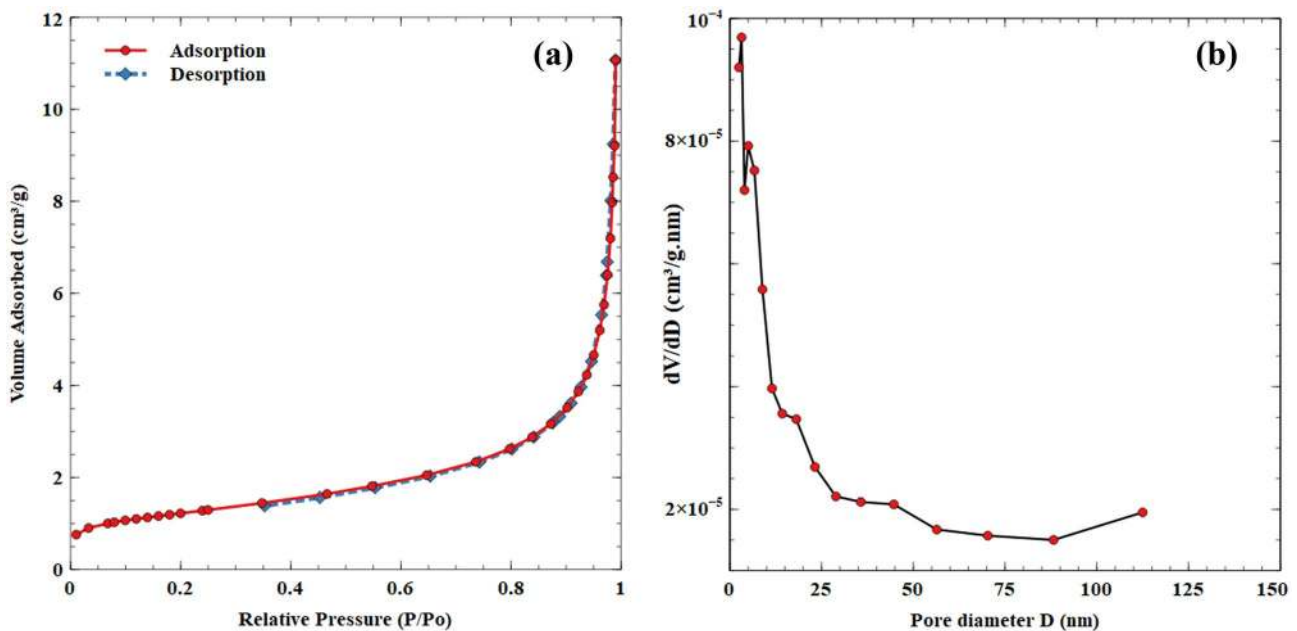


Fig. 4 (a) N₂ adsorption–desorption isotherm and (b) pore size distribution of synthesized CaO nanocrystalline particles

using Scherrer formula from Eq. (3) [18]. The average crystallite size of CaO and CaCO₃ was 100 ± 20 nm and Ca(OH)₂ was 5 nm. Also, the weight percentage of CaO nanocrystalline particles decrease from 73.71 to 66.62% after 1 month in characterization.

Brunauer–Emmett–Teller (BET)

The specific surface area and the distribution of pore sizes of the CaO-NPs calcined at 650 °C were examined from N₂ gas adsorption–desorption measurements. Figure 4a describes the N₂ adsorption isotherm of type III hysteresis, which is characteristic of microporous materials [36]. From the Barrett–Joyner–Halenda (BJH) pore-size distribution plot (Fig. 4b), the estimated average pore diameter was found to be 21.5062 nm. The BET surface area, micropore area, and micropore volume were 4.3439 m²/g, 0.8627

m²/g, and 0.000371 cm³/g, respectively. It can be classified that most of the pores are mesopores (pore sizes between 2 and 50 nm), which is matched with the literature of N. Tangboriboon et al. [37] and Zahra Mirghiasi et al. [18].

Mechanical characterization

Tensile strength

The tensile stress–strain response of ultrasonic and without ultrasonic has been shown in Fig. 5a. In each set, three samples were tested for both cases, the average of the tensile test are presented in Fig. 5a for both mixing. A great improvement has been seen in the % modulus, and decrement in the tensile strength and % failure strain are observed, as the CaO content increases from 0 to 8 wt%. Also, the tensile modulus of neat EPDM and its nanocomposites were measured which is

Fig. 5 (a) Tensile stress values of neat EPDM rubber and its nanocomposites with and without ultrasonic mixing. (b) Tensile modulus values of neat EPDM rubber and its nanocomposites with and without ultrasonic mixing

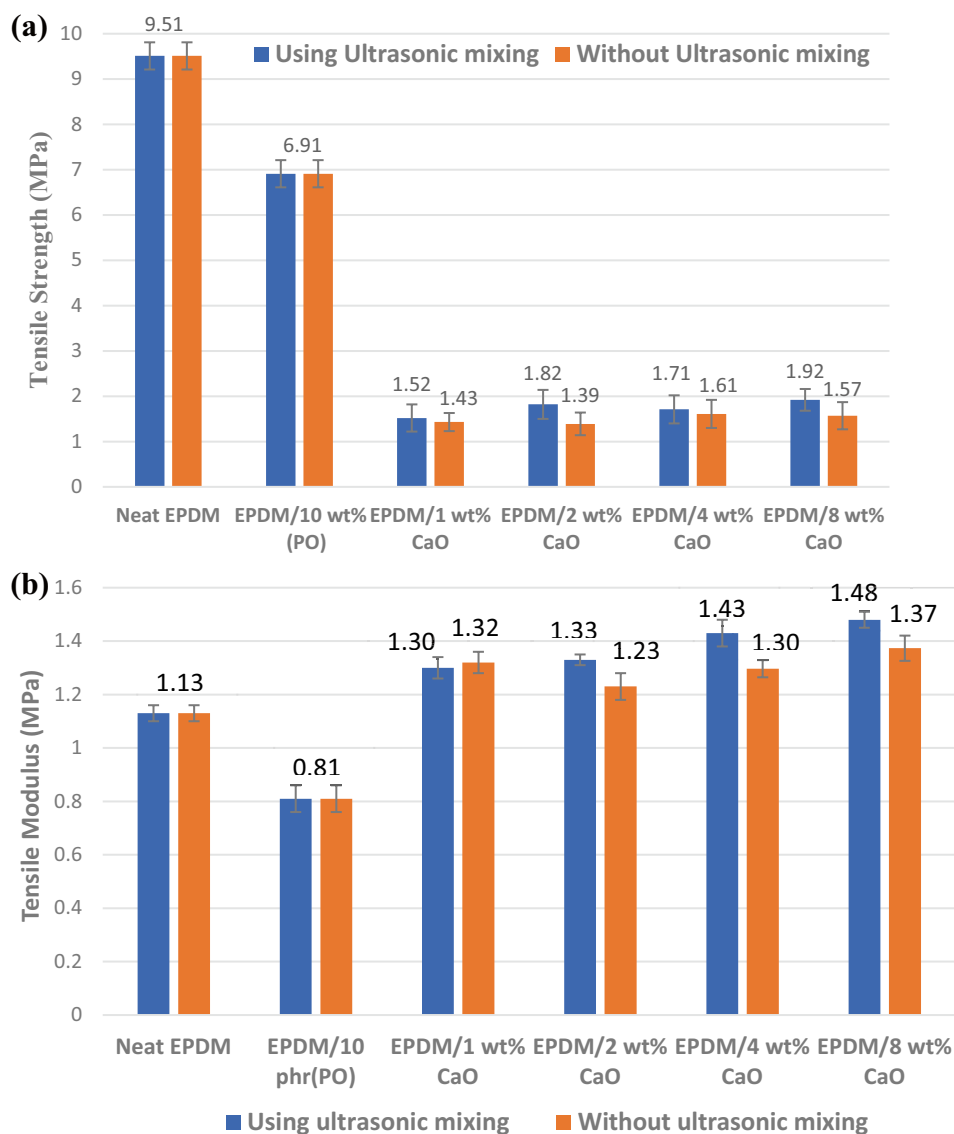
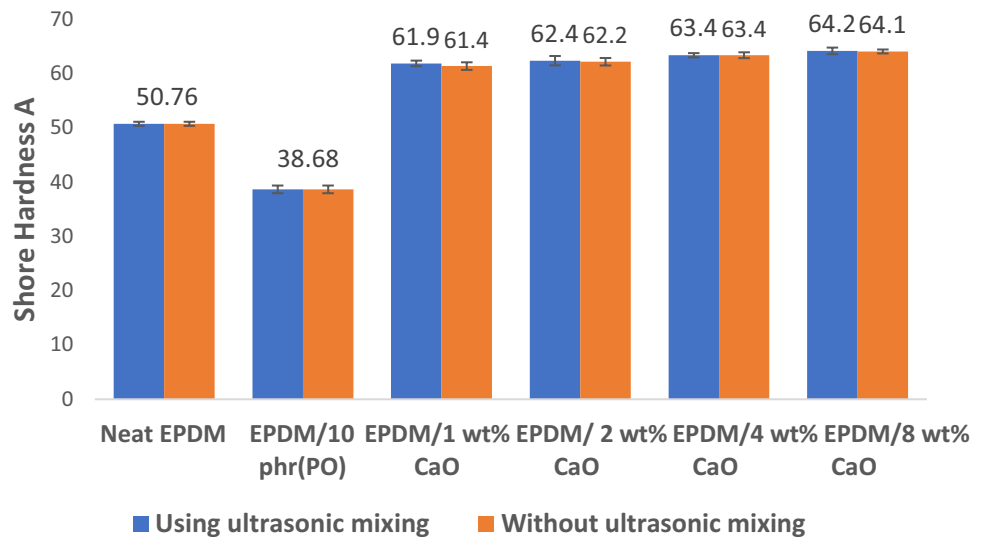


Fig. 6 Shore hardness of neat EPDM rubber and its nanocomposites. Using ultrasonic mixing and without ultrasonic mixing



presented in Fig. 5b for both cases. It revealed that the maximum % modulus that has been shown by using ultrasonic mixing was 24% and without ultrasonic mixing was 18% higher than neat EPDM for 8 wt% of CaO, due to stiffening of EPDM structure by adding CaO particles. The behavior of the ultrasonic treated sample is better due to the more homogeneous distribution of the CaO, and the formation of agglomerates is avoided, as one can observe on Fig. 11. The CaO particles were agglomerated without ultrasonic treatment (Fig. 11a, c), but using ultrasonic mixing, the formation of agglomeration of CaO could be avoided, and the particles were well dispersed (Fig. 11b, d); therefore, tensile strength is higher compared with the samples without ultrasonic treatment [42].

The tensile strength decreases by adding CaO nanocrystalline particles, which is agreed with the literature [38, 39] [44, 45]. In the literature of Wang et al. [30], they studied thermal mechanical properties of EPDM rubber with different amounts of nano ZnO reinforced. Nano ZnO particles enhance better dynamic heat build-up mechanical properties by in situ modification. Also, from the literature of Su et al. [40], they investigated mechanical, electrical, and cure properties of EPDM mixed with Sm_2O_3 . Furthermore, rubber filled with KH845-4-treated Sm_2O_3 had higher tensile and tear strength than rubber filled with SG-Si602-treated Sm_2O_3 . This is due to the possibility of sulfuric atoms participating in the peroxide-cured system. But

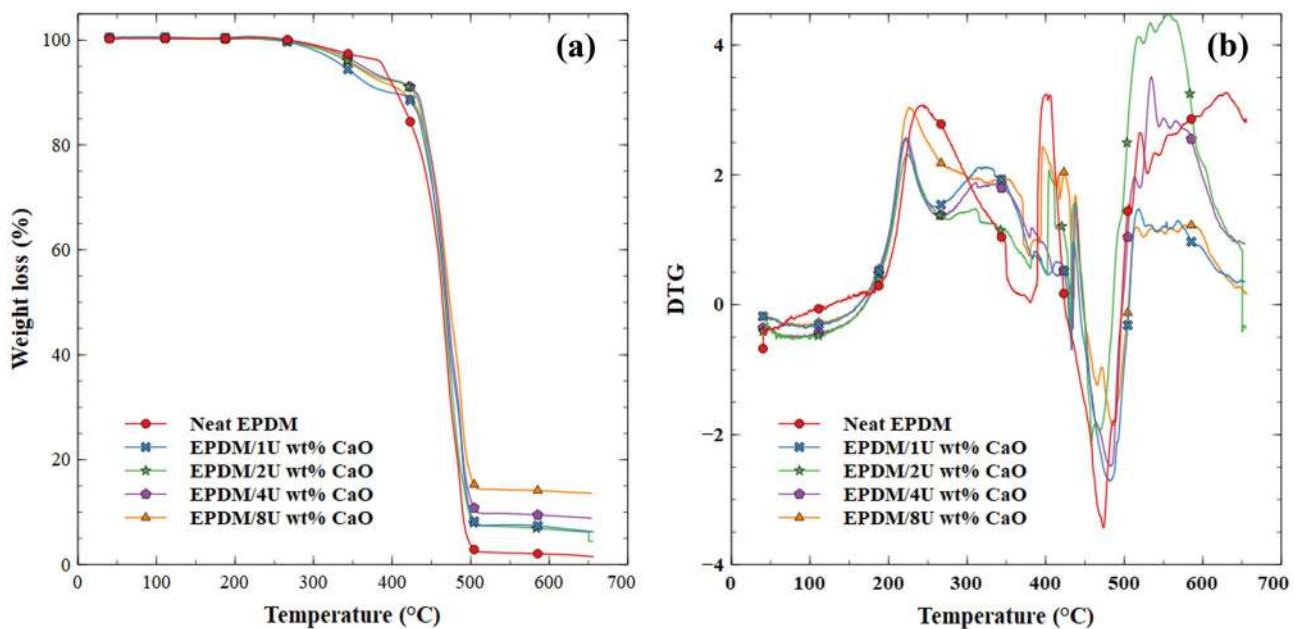


Fig. 7 (a) TGA curve and (b) DTG curve for neat EPDM rubber and its nanocomposites using ultrasonic mixing

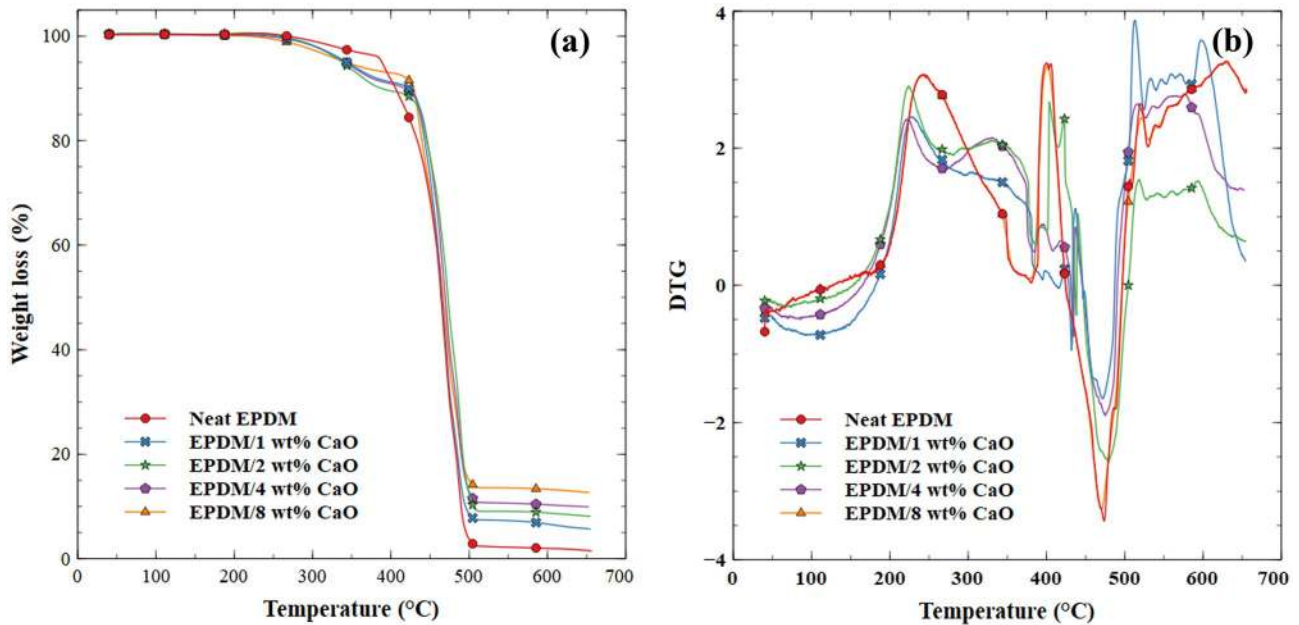


Fig. 8 (a) TGA curve and (b) DTG curve for neat EPDM rubber and its nanocomposites without using ultrasonic mixing

SG-Si₆O₂-treated Sm₂O₃ has maximum hardness. Mishra [41] studied mechanical and thermal properties of EPDM rubber filled with nano CaCO₃, commercial CaCO₃, and fly ash. Mechanical properties such as tensile strength and elongation at break increase with increasing amount of filler especially calcium carbonate nanocrystalline particles have better result comparing with commercial CaCO₃ and fly ash. Nanocrystalline particles showed appreciable result.

Hardness test

Figure 6 revealed that the hardness of the materials increases with adding CaO nanocrystalline particles, and the graph showed hardness of matrix gradually increases by adding the particles for both cases, with ultrasonic and without ultrasonic mixing. The maximum hardness observed in 8 wt% of CaO particles for both cases

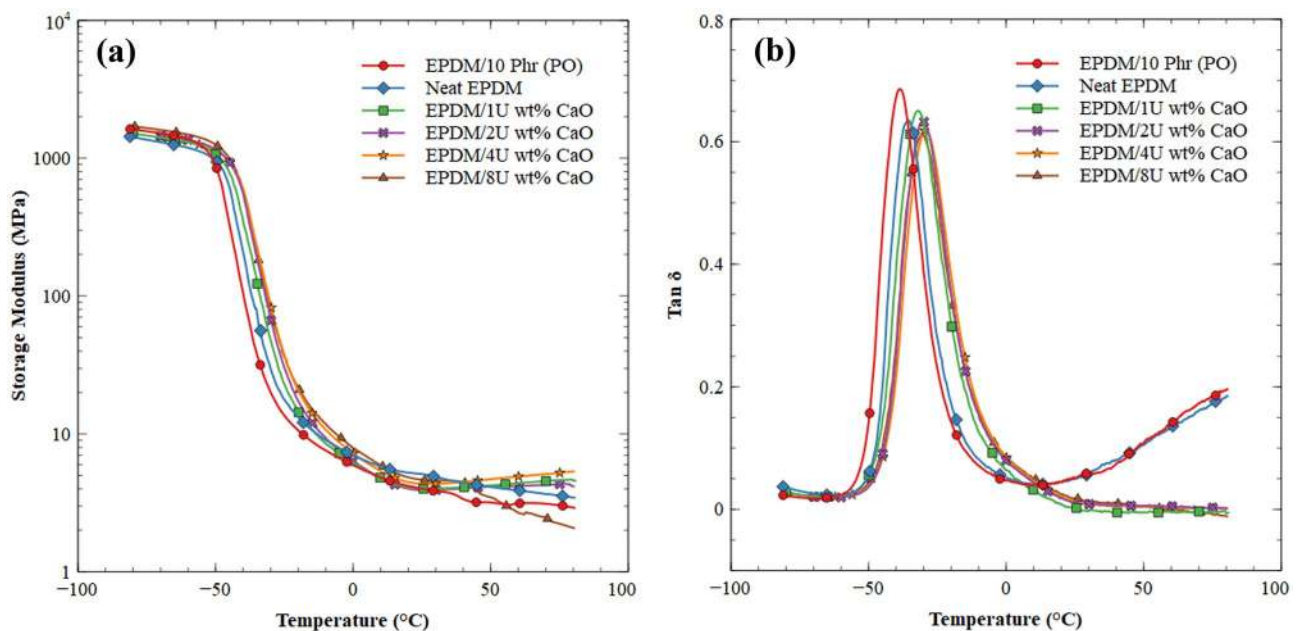


Fig. 9 (a) Storage modulus; (b) loss factor ($\tan \delta$) for neat EPDM and its nanocomposites using ultrasonic mixing

Table 2 TGA properties for neat EPDM rubber and its nanocomposites using ultrasonic mixing

Material	Initial temperature 40 °C		Final temperature 655 °C		DTG Peak (°C)
	Initial weight (mg)	%wt remaining	Final weight (mg)	%wt remaining	
Neat EPDM	60.3	100	0.897	1.48	473
EPDM/1U wt% CaO	32.59	100	2.028	6.22	479
EPDM/2U wt% CaO	46.96	100	2.896	6.16	471
EPDM/4U wt% CaO	46.96	100	3.975	8.46	480
EPDM/8U wt% CaO	38.04	100	5.173	13.60	481

with ultrasonic and without ultrasonic mixing was 64.2 and 64.1, respectively; almost both cases have the same hardness about 26% higher than neat EPDM. From the literature of Su et al. [40], they investigated mechanical, electrical, and cure properties of EPDM mixed with Sm_2O_3 . SG- Si_6O_2 -treated Sm_2O_3 has maximum hardness. Aguilera-Camacho et al. [43] investigated the effect of CaO nanocrystalline particles on microhardness and tribological properties of poly(methyl methacrylate) coating; it prepared via in situ polymerization adding 0.05 wt% CaO nanocrystalline particles to the PMMA matrix, the result showed by using CaO nanocrystalline particles to PMMA hardness increase. Hamza [44] studied mechanical properties and thermal aging of EPDM with different amounts of high abrasion furnace (HAF) carbon black. It was observed that hardness increases with an increasing amount of carbon black.

Thermal analysis

Thermogravimetric analysis (TGA)

The temperature correlated with the derivative curve's peak value estimates the thermal stability of nanocomposites and neat EPDM rubber. The higher the peak temperature, the better the thermal stability. Figures 7a, 8a represent the TGA curves for neat EPDM, and different weight contents of CaO particles included EPDM samples for both cases. It is revealed from Figs. 7a, 8a that the %wt loss is higher for neat EPDM rubber, while wt% is lower for CaO/EPDM nanocomposite as increasing the temperature from 40 to

655 °C for both cases using or without using ultrasonic mixing. It is observed from derivative thermogravimetry (DTG) peak curve especially for ultrasonic mixing which represents from Table 2 and Fig. 7b derivative peak temperature increase with adding of CaO to EPDM rubber, the maximum peak temperature revealed by adding 8 wt% of CaO. In conclusion, the thermal stability increases with the dispersion of CaO particles. It is observed from Table 2 using ultrasonic mixing that the overall %wt loss at 655 °C is 98.52%, 93.78%, 93.84% 91.54%, and 86.4% for neat EPDM rubber, 1 wt%, 2 wt%, 4 wt%, and 8 wt% nanocomposites, respectively. Derivative thermogravimetry (DTG) peak curve without using ultrasonic mixing represents in Table 3 and Fig. 8b; the maximum peak temperature revealed by adding 2 wt% of CaO. Also, it is observed from Table 3 without using ultrasonic mixing that the overall %wt loss at 655 °C is 98.52%, 94.31%, 991.9% 90.07%, and 87.34% for neat EPDM rubber, 1 wt%, 2 wt%, 4 wt%, and 8 wt% nanocomposites, respectively. This confirms that CaO addition to EPDM led to protecting EPDM structure against thermal degradation. It is supposed that the reason of thermal degradation of EPDM is the presence of acidic decomposition products of peroxide crosslinking agent. Radical decomposition of peroxide takes place only in a basic environment. The better is the dispersion of CaO, the less is the probability of areas of the thermal degradation.

Dynamic mechanical analysis (DMA)

The thermomechanical behavior of the samples was characterized by the use of DMA over a temperature range

Table 3 TGA properties for neat EPDM rubber and its nanocomposites without ultrasonic mixing

Material	Temperature 40 °C		Temperature 655 °C		DTG peak (°C)
	Initial weight (mg)	%wt remaining	Final weight (mg)	%wt remaining	
Neat EPDM	60.3	100	0.8974	1.48	473
EPDM/1 wt% CaO	44.92	100	2.5597	5.69	470
EPDM/2 wt% CaO	37.49	100	3.0371	8.10	476
EPDM/4 wt% CaO	46.65	100	4.6341	9.93	475
EPDM/8 wt% CaO	56.18	100	7.1174	12.66	469

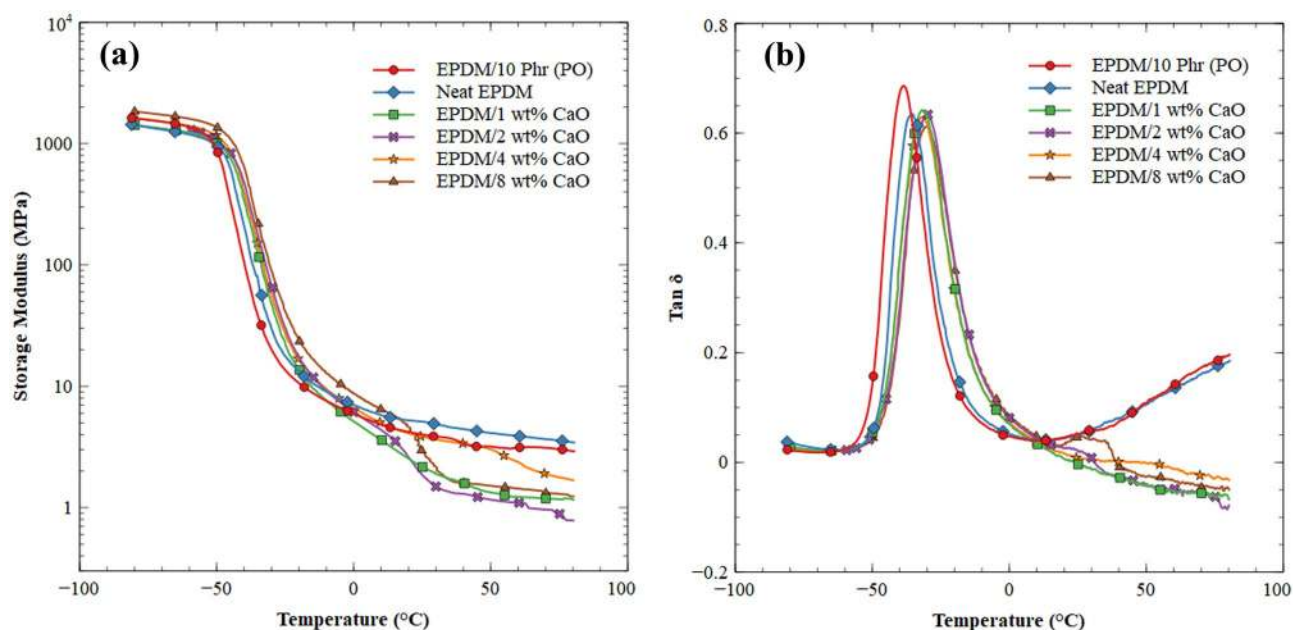


Fig. 10 (a) Storage modulus; (b) loss factor ($\tan \delta$) for neat EPDM and its nanocomposites without ultrasonic mixing

of -80 to 80 °C with a heating rate of 2 °C per minute at a frequency of 10 Hz. The thickness and width of the tensile samples used were ≈ 1 mm and ≈ 10 mm, respectively; also the gauge length of the specimen used was 15 mm. Calculations were performed with the measured dimensions. It is important to use a low heating

rate so that the sample can have enough time to achieve the thermal balance within the chamber. As a function of temperature, the storage modulus and the $\tan(\delta)$ /loss factor were measured. Glass transition temperature (T_g) were determined at the maximum point of \tan /loss tangent as shown in Figs. 9b, 10b which is denoted in

Fig. 11 SEM micrographs for EPDM rubber mixed with CaO particles (a,c) without ultrasonic mixing (b,d) using ultrasonic mixing. (Nominal magnification is 5 k \times)

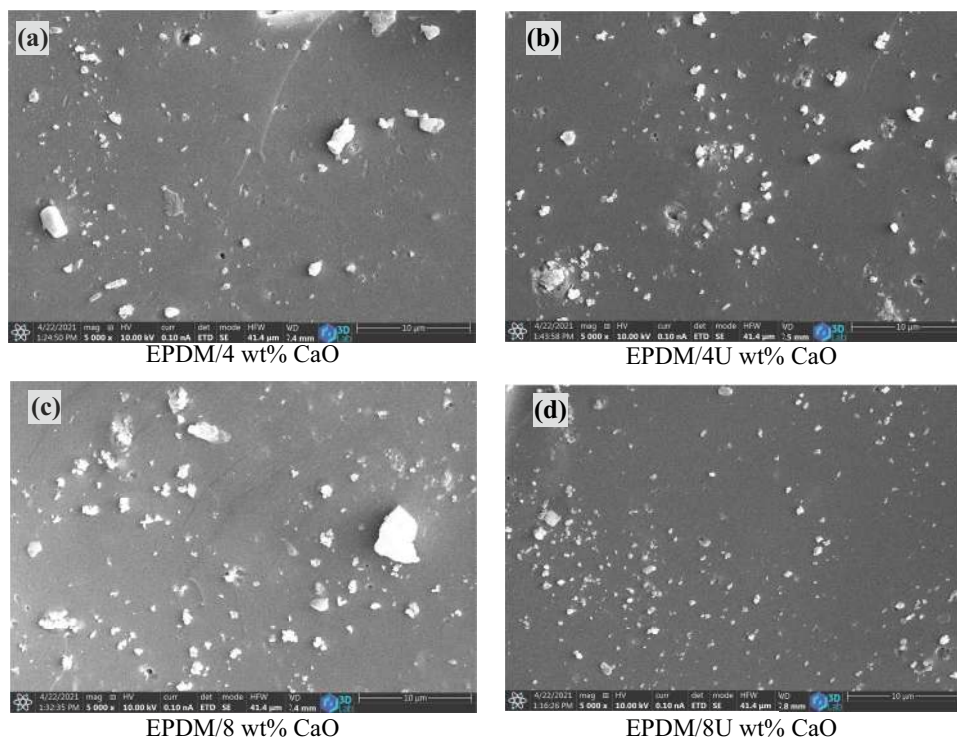


Table 4 Glass transition temperature for Neat EPDM and its nanocomposites, with or without ultrasonic mixing

Sample	Glass transition temperature (T_g) °C using ultrasonic mixing	Glass transition temperature (T_g) °C without ultrasonic mixing
Neat EPDM	-35.2	-35.2
EPDM/10 wt% PO	-39.05	-39.05
EPDM/1 wt% CaO	-31.95	-31.8
EPDM/2 wt% CaO	-30.4	-29.75
EPDM/4 wt% CaO	-28.95	-31.35
EPDM/8 wt% CaO	-29.85	-29.7

Table 4 using ultrasonic mixing and without ultrasonic mixing. Figures 9a, 10a illustrate the effect of temperature on the storage modulus for both cases. The viscoelastic behavior of the matrix or composites is classified into three regions: glassy, transitional, and rubbery. The result revealed that storage modulus decreases as a function of temperature because of material further goes into a rubber state by increasing temperature. The decrease in storage modulus as temperature increases is visible in Figs. 9a, 10a, for both cases; also a dramatic drop was observed in the glass transition region due to segmental mobility of the EPDM rubber, around -39 °C to -28 °C. Some researchers corresponding loss tangent ($\tan \delta$) peak as glass transition temperature [29, 45]. The glass transition temperature in the present study is denoted in Table 4 for both cases. The result indicated that glass transition temperature increases with adding CaO nanocrystalline particles to the matrix for both cases, and the maximum (T_g) showed in 1 wt% CaO for the ultrasonic mixing. The thermal stability increases with adding CaO particles to the EPDM rubber. In the literature of Mohamed et al. [27] who investigated the effect of CaO particles on the properties of polyamide 6 (PA 6) by adding 0.5% calcium oxide, CaO nanocrystalline particles improved the thermal stability of the composite. Rana et al. [29] studied electrical, mechanical, and thermal properties of EPDM rubber with different amounts of MMT nano clay reinforced (2 wt%, 4wt%, and 6 wt%); the higher value of thermal stability is observed in 2 wt%. Mishra [41] studied mechanical and thermal properties of EPDM rubber filled with nano CaCO_3 , commercial CaCO_3 , and fly ash. Synthesizing nanoparticles done by solution spray, thermal properties improved, and nano CaCO_3 is more stable than the other; flame retardancy increase with the amount of filler, and nanoparticles showed appreciable result.

Scanning electron microscopy (SEM) analysis for composite

SEM micrographs of EPDM/CaO composite were taken at a constant scale of $10 \mu\text{m}$ to see the CaO dispersion in EPDM rubber. The composites are presented in Fig. 11a, c without using ultrasonic mixing and Fig. 11b, d with using ultrasonic mixing. The SEM result revealed that using ultrasonic mixing has a great influence on the dispersion of CaO particle compared to non-using of the ultrasonic mixing; without ultrasonic mixing, it's obvious in Fig. 11a, c that CaO particles were agglomerated. Also, the best mixing by ultrasonic improved the dispersity and decreased the agglomeration which was showed in 4 wt% and 8 wt% of CaO particles from Fig. 11b, d. As a consequence, higher tensile via using ultrasonic mixing is revealed compared to non-using of ultrasonic mixing as shown in Fig. 5.

Volume resistivity

The measurements of volume resistivity were observed of neat EPDM rubber and the nanocomposites. The dielectric strength, dielectric constant, and surface and volumetric resistance are the key electrical properties that identify the properties of an insulating material. The resistance of the specimen was so high that the measurement was not possible. Therefore, new and specific electrode was made as shown in Fig. 1 to measure the volume resistivity. In the present study, volumetric resistivities were evaluated by applying 1 kV to the surfaces of the samples for 60 s; the plate was 1 mm thick. The calculated and comparative measurement

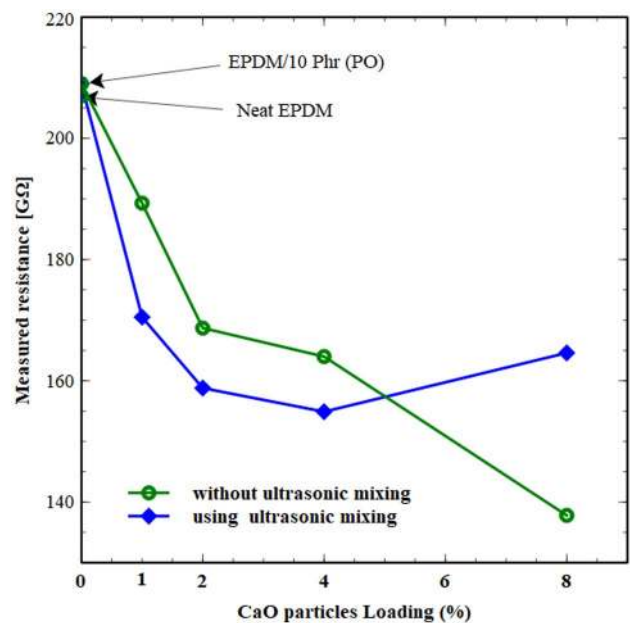
**Fig. 12** Measured resistance of neat EPDM and its nanocomposites

Table 5 Measured resistance for EPDM and its nanocomposite

Specimen	R_{measured} [G Ω]	$R_{\text{calculated}}$ [G Ω]	ρ [$\Omega\cdot\text{cm}$] (approx.)
EPDM/10 wt% PO	209	not evaluable	-
Neat EPDM	207	not evaluable	-
EPDM/0 wt% CaO	182.5	1542	$1.08\cdot 10^{15}$
EPDM/1 wt% CaO	189.3	2214	$1.55\cdot 10^{15}$
EPDM/1U wt% CaO	170.5	967	$6.76\cdot 10^{14}$
EPDM/2 wt% CaO	168.7	912	$6.38\cdot 10^{14}$
EPDM/2U wt% CaO	158.8	682	$4.97\cdot 10^{14}$
EPDM/4 wt% CaO	164.0	789	$5.52\cdot 10^{14}$
EPDM/4U wt% CaO	154.9	615	$4.90\cdot 10^{14}$
EPDM/8 wt% CaO	137.8	412	$2.88\cdot 10^{14}$
EPDM/8U wt% CaO	164.6	804	$5.62\cdot 10^{14}$

is explained in Table 5. The resistance of blade electrode system (R_1) is 201 G Ω which is parallel to the resistance to be measured (R_2). For parallel resistance

$$\frac{1}{R} = \frac{1}{R_1} + \frac{1}{R_2} \text{ is valid or } R = R_1 \times R_2 \text{ by other notaion} \quad (4)$$

Because R was measured, the resistance of the sample can be calculated as:

$$R_2 = \frac{1}{\frac{1}{R} - \frac{1}{R_1}} \quad (5)$$

Comparative measurement was carried out with a plasticized PVC plate. Its specific volume resistance was $\rho = 1.92\cdot 10^{12}$ [$\Omega\cdot\text{cm}$]. The measured resistance was 173.2 G Ω . From this data, the equivalent A/l is 700 cm. However, its accuracy is not better than $\pm 20\%$. The values in the last column were calculated by this A/l value.

Remark: Calculating with the smallest specific volume resistivity (EPDM/8 wt% CaO) the resistance with the standard arrangement (10 cm² electrode and about 1.4 mm thickness) the resistance would be about 4 T Ω ; well over the top limit of the instrument.

The result observed from Table 5 and Fig. 12 that by adding CaO nanocrystalline particles to EPDM rubber, the volume resistivity and measured resistivity of EPDM gradually decreases in both cases. Because of the low resistivity, EPDM with 8 wt% of CaO is suitable for use in insulating applications. In the literature of Zonghuan Li, et al. [46], the effect of different carbon black structures on the electrical properties of filled EPDM rubber revealed that adding carbon black is useful for insulating purpose. Also cure, mechanical, and electrical properties of EPDM filled with Sm₂O₃ and treated with various coupling agents were compared in the literature of Su et al. [40]. The result revealed that by adding Sm₂O₃ to EPDM rubber, volume resistivity decreases. The EPDM composites are extremely good insulators.

Conclusion

The calcium oxide nanocrystalline particles were successfully synthesized by the precipitation method. SEM revealed that the nanocrystalline particles mostly spherical and the average particle size is about 280 nm. From BET analysis, surface area, micropore area, and micropore volume were 4.3439 m²/g, 0.8627 m²/g, and 0.000371 cm³/g, respectively. It can be classified that most of the pores are mesopores (pore sizes between 2 and 50 nm). Also, XRD analysis indicates that the average crystallite size of CaO and CaCO₃ was 100 ± 20 nm, and Ca (OH)₂ was 5 nm. Also, the weight percentage of CaO nanocrystalline particles decrease from 73.71 to 66.62% after 1 month in characterization. The experimental results obtained from the thermal, electrical, and mechanical characterization of composites using ultrasonic are:

- 1- Using ultrasonic mixing as a pre-mixing has a great influence on the dispersion of CaO nanocrystalline particles in the EPDM rubber matrix.
- 2- Using ultrasonic mixing revealed a great improvement in the mechanical and thermal properties of EPDM rubber by adding CaO nanocrystalline particles. The tensile modulus and hardness gradually increased by adding CaO nanocrystalline particles. From DMA and TGA measurement, the thermal stability of the rubber matrix was increased by adding CaO nanocrystalline particles.
- 3- Interesting observation that the ultrasonically mixed CaO containing sheets were not rugged.
- 4- Volume resistivity gradually decrease with increasing CaO nanocrystalline particles.

Acknowledgements The authors are appreciative for the help provided by Dr. Tamás Szabo and Miss. Ei Ei Khine for their constant help during some stages of work. I want to thank Dr. Daniel Koncz-Horvath for the SEM investigation, Mr. Tibor Ferenczi for the BET investigation, Dr. Ferenc Kristály for the XRD investigation, and Dr. Tamas Szabo for

the DMA investigation. The authors are thankful to one of the unidentified reviewers for his/her important comments, which considerably improved this paper.

Funding Open access funding provided by University of Miskolc.

Declarations

Conflict of interest The authors declare no competing interests.

Open Access This article is licensed under a Creative Commons Attribution 4.0 International License, which permits use, sharing, adaptation, distribution and reproduction in any medium or format, as long as you give appropriate credit to the original author(s) and the source, provide a link to the Creative Commons licence, and indicate if changes were made. The images or other third party material in this article are included in the article's Creative Commons licence, unless indicated otherwise in a credit line to the material. If material is not included in the article's Creative Commons licence and your intended use is not permitted by statutory regulation or exceeds the permitted use, you will need to obtain permission directly from the copyright holder. To view a copy of this licence, visit <http://creativecommons.org/licenses/by/4.0/>.

References

- Hamed GR (2000) Reinforcement of rubber. *Rubber Chem Technol* 73:524–533
- Pandey JK, Reddy KR, Kumar AP, Singh R (2005) An overview on the degradability of polymer nanocomposites. *Polym Degrad Stab* 88:234–250
- Zheng H, Zhang Y, Peng Z, Zhang Y (2004) Influence of clay modification on the structure and mechanical properties of EPDM/montmorillonite nanocomposites. *Polym Test* 23:217–223
- Guan Y, Zhang L-X, Zhang L-Q, Lu Y-L (2011) Study on ablative properties and mechanisms of hydrogenated nitrile butadiene rubber (HNBR) composites containing different fillers. *Polym Degrad Stab* 96:808–817
- Avella M, Errico ME, Martuscelli E (2001) Novel PMMA/CaCO₃ nanocomposites abrasion resistant prepared by an in situ polymerization process. *Nano Lett* 1:213–217
- Wetzel B, Hauptert F, Friedrich K, Zhang MQ, Rong MZ (2002) Impact and wear resistance of polymer nanocomposites at low filler content. *Polym Eng Sci* 42:1919–1927
- Frounchi M, Dadbin S, Salehpour Z, Noferesti M (2006) Gas barrier properties of PP/EPDM blend nanocomposites. *J Membr Sci* 282:142–148
- Li Z, Zhang J, Chen S (2008) Effects of carbon blacks with various structures on vulcanization and reinforcement of filled ethylene-propylene-diene rubber. *Express Polym Lett* 2:695–704
- Vittayakorn W, Bunjong D, Muanghlua R, Vittayakorn N (2011) Characterization and properties of BaTi 3O 3/MgO nanocomposite ceramics
- Oskam G (2006) Metal oxide nanoparticles: synthesis, characterization and application. *J Sol-Gel Sci Technol* 37:161–164
- Keller AA et al (2010) Stability and aggregation of metal oxide nanoparticles in natural aqueous matrices. *Environ Sci Technol* 44:1962–1967
- Roy A, Bhattacharya J (2011) Microwave-assisted synthesis and characterization of CaO nanoparticles. *Int J Nanosci* 10:413–418
- Tang Z-X, Claveau D, Corcuff R, Belkacemi K, Arul J (2008) Preparation of nano-CaO using thermal-decomposition method. *Mater Lett* 62:2096–2098
- Ngamcharussrivichai C, Meechan W, Ketcong A, Kangwansaichon K, Butnark S (2011) Preparation of heterogeneous catalysts from limestone for transesterification of vegetable oils—Effects of binder addition. *J Ind Eng Chem* 17:587–595
- Amin Alavi M, Morsali A (2010) Ultrasonic-assisted synthesis of Ca (OH) 2 and CaO nanostructures. *J Exp Nanosci* 5:93–105
- Park HK, Bae MW, Nam IH, Kim S-G (2013) Acid leaching of CaOSiO₂ resources. *J Ind Eng Chem* 19:633–639
- Liu T, Zhu Y, Zhang X, Zhang T, Zhang T, Li X (2010) Synthesis and characterization of calcium hydroxide nanoparticles by hydrogen plasma-metal reaction method. *Mater Lett* 64:2575–2577
- Mirghiasi Z, Bakhtiari F, Darezereshki E, Esmailzadeh E (2014) Preparation and characterization of CaO nanoparticles from Ca (OH) 2 by direct thermal decomposition method. *J Ind Eng Chem* 20:113–117
- Madhusudhana N, Yogendra K, Mahadevan K (2012) Decolorization of coralene dark red 2B azo dye using calcium oxide nanoparticle as an adsorbent. *Int J Res Chem Environ* 2:21–25
- Roy A, Gauri SS, Bhattacharya M, Bhattacharya J (2013) Antimicrobial activity of CaO nanoparticles. *J Biomed Nanotechnol* 9:1570–1578
- Sadeghi M, Husseini MH (2013) A novel method for the synthesis of CaO nanoparticle for the decomposition of sulfurous pollutant. *Journal of Applied Chemical Research* 7:39–49
- Darčanova O., Beganskienė A, Kareiva A (2015) Sol-gel synthesis of calcium nanomaterial for paper conservation. *chemija*. 26: 25–31
- Charles A. Harper, Edward M. Petrie (2003) *Plastic materials and processes*. John Wiley & Sons, Inc., Hoboken, New Jersey, Canada, pp 170–171.
- Jia X et al (2008) Effects of pretreated polysulfonamide pulp on the ablation behavior of EPDM composites. *Mater Chem Phys* 112:823–830
- Shokrzadeh A, Naderi G, Esmizadeh E (2014) Mechanical and rheological properties of calcium carbonate-filled ethylene propylene diene elastomer reinforced by metallic acrylate salt. *Fibers and Polymers* 15:1694–1700
- Contreras JE, Rodriguez EA, Taha-Tijerina J (2018) "Recent trends of nanomaterials for high-voltage applications," in *Handbook of Nanomaterials for Industrial Applications*
- Mohamed W, Nasr H, Gutmann R, Sobh R (2015) Effect of CaO nanoparticles on the properties of polyamide 6. *J Egy Chem* 58:365
- Sunil J, Vignesh J, Vettumperumal R, Maheswaran R, Raja RA (2019) The thermal properties of CaO-nanofluids. *Vacuum* 161:383–388
- Rana AS, Vamshi MK, Naresh K, Velmurugan R, Sarathi R (2020) Mechanical, thermal, electrical and crystallographic behaviour of EPDM rubber/clay nanocomposites for out-door insulation applications. *Advances in Materials and Processing Technologies* 6:54–74
- Wang Z, Lu Y, Liu J, Dang Z, Zhang L, Wang W (2010) Preparation of nano-zinc oxide/EPDM composites with both good thermal conductivity and mechanical properties. *J Appl Polym Sci* 119:1144–1155
- Brown R (2002) *Handbook of polymer testing*. Rapra Technology Limited, Crewe, UK
- Grellmann W (2007) *Polymer testing*. Carl Hanser Verlag, munich
- Rodriguez F (2003) *Principles of Polymer Systems*. Taylor & Francis Books, Inc., 29 West 35th Street, New York, NY 10001

34. Ruiz J-RR, Parelló TC, Gómez RC (2016) Identification of NR and EPDM samples by means of thermogravimetric analysis and multivariate methods. *IEEE Sens J* 16:7705–7712
35. Nikulshina V, Galvez M, Steinfeld A (2007) Kinetic analysis of the carbonation reactions for the capture of CO₂ from air via the Ca(OH)₂–CaCO₃–CaO solar thermochemical cycle. *Chem Eng J* 129:75–83
36. Sing KSW (1985) Reporting physisorption data for gas/solid systems with special reference to the determination of surface area and porosity (Recommendations 1984). *Pure Appl Chem* 57:603–619. <https://doi.org/10.1351/pac198557040603>
37. Tangboriboon N, Kunanuruksapong R, Sirivat A (2012) Preparation and properties of calcium oxide from eggshells via calcination. *Mater Sci-Pol* 30:313–322
38. Ma LX, Zhang N, Yang G, He Y (2013) "Thermal conductivity of EPDM rubber filled with modified nano-AlN," in *key engineering materials*, vol. 561: Trans Tech Publ, pp. 146–151.
39. Anuar J, Mariatti M, Ismail H (2007) Study on tensile, electrical, and thermal properties of aluminium particle filled natural rubber (NR) and ethylene-propylene-diene terpolymer (EPDM) composites. *Polym-Plast Technol Eng* 46:1201–1206
40. Su J, Chen S, Zhang J, Xu Z (2009) Comparison of cure, mechanical, electric properties of EPDM filled with Sm₂O₃ treated by different coupling agents. *Polym Test* 28:235–242
41. Mishra S, Patil U, Shimpi N (2009) Synthesis of mineral nanofiller using solution spray method and its influence on mechanical and thermal properties of EPDM nanocomposites. *Polym-Plast Technol Eng* 48:1078–1083
42. Sallal HA, Abdul-Hamead AA, Othman FM (2020) Effect of nano powder (Al₂O₃-CaO) addition on the mechanical properties of the polymer blend matrix composite. *Defence Technology* 16:425–431
43. Aguilera-Camacho L, Hernández-Navarro C, Moreno K, García-Miranda J, Arizmendi-Morquecho A (2015) Improvement effects of CaO nanoparticles on tribological and microhardness properties of PMMA coating. *J Coat Technol Res* 12:347–355
44. Hamza S (1998) Effect of aging and carbon black on the mechanical properties of EPDM rubber. *Polym Test* 17:131–137
45. Portella EH, Romanzini D, Angrizani CC, Amico SC, Zattera AJ (2016) Influence of stacking sequence on the mechanical and dynamic mechanical properties of cotton/glass fiber reinforced polyester composites. *Mater Res* 19:542–547
46. Li Z, Zhang J, Chen S (2009) Effect of carbon blacks with various structures on electrical properties of filled ethylene-propylene-diene rubber. *J Electrostatics* 67:73–75

Publisher's Note Springer Nature remains neutral with regard to jurisdictional claims in published maps and institutional affiliations.